HHS Public Access

Author manuscript

Integr Biol (Camb). Author manuscript; available in PMC 2015 July 24.

Published in final edited form as:

Integr Biol (Camb). 2014 July 24; 6(7): 673–684. doi:10.1039/c4ib00050a.

Dynamics and evolution of β-catenin-dependent Wnt signaling revealed through massively parallel clonogenic screening

Pavak K. Shah[a], **Matthew P. Walker**[b], **Christopher E. Sims**[c], **Michael B. Major**[b,d], and **Nancy L. Allbritton**[a,c,d,*]

[a]Department of Biomedical Engineering, University of North Carolina, Chapel Hill, NC 27599, USA and North Carolina State University, Raleigh, USA

[b]Department of Cell Biology and Physiology, University of North Carolina, Chapel Hill, NC 27599, USA

[c]Department of Chemistry, University of North Carolina, Chapel Hill, USA

[d]Lineberger Comprehensive Cancer Center, University of North Carolina, Chapel Hill, USA

Abstract

Wnt/β-catenin signaling is of significant interest due to the roles it plays in regulating development, tissue regeneration and disease. Transcriptional reporters have been widely employed to study Wnt/β-catenin signal transduction in live cells and whole organisms and have been applied to understanding embryonic development, exploring oncogenesis and developing therapeutics. Polyclonal heterogeneity in reporter cell lines has historically been seen as a challenge to be overcome in the development of novel cell lines and reporter-based assays, and monoclonal reporter cell lines are commonly employed to reduce this variability. A375 cell lines infected with a reporter for Wnt/β-catenin signaling were screened over short (< 6) and long (> 25) generational timescales. To characterize phenotypic divergence these time-scales, a microfabricated cell array-based screen was developed enabling characterization of 1,119 clonal colonies in parallel. This screen revealed phenotypic divergence after <6 generations at a similar scale to that observed in monoclonal cell lines cultured for >25 generations. Not only were reporter dynamics observed to diverge widely, but monoclonal cell lines were observed with seemingly opposite signaling phenotypes. Additionally, these observations revealed a generational-dependent trend in Wnt signaling in A375 cells that provide insight into the pathway's mechanisms of positive feedback and self-inhibition.

Introduction

Wnt/β-catenin signaling is an evolutionarily conserved signaling pathway that is involved in development, adult tissue homeostasis, tissue regeneration, and disease. In the absence of

*nlallbri@unc.edu.

Electronic Supplementary Information (ESI) available: Microraft array fabrication; Micropallet array fabrication; P-values for all two-tailed Wilcoxon rank sum tests; Comparison of reagent consumption and clonal yield of screening for arrays versus conventional methods; Single cell traces of the kinetics of mCherry fluorescence; Comparisons between measured parameters from single-cell tracking.

Wnt ligand signaling, β-catenin levels are kept low through ubiquitination and proteosome-dependent degradation. Specifically, cytosolic β-catenin is captured by a complex of proteins comprising GSK3β, CK1a, APC and AXIN, which promote its phosphorylation and subsequent ubiquitination by the β-TrCP ubiquitin ligase. Binding of the Wnt ligand to the frizzled receptor inhibits GSK3b-dependent phosphorylation of b-catenin, leading to increased b-catenin levels and stability. β-catenin is then translocated to the nucleus and acts as a co-activator for TCF/LEF family transcription factors. Wnt signaling interacts with a large number of signaling pathways in normal and pathological contexts and large-scale screening efforts continue to identify many novel regulators and potential therapeutic targets.[1–4] The importance of single-cell measurements in the study of tumor systems and signaling pathways has been highlighted by the observation of significant heterogeneity in Wnt signaling at the single-cell level in primary tumor-derived spheroid cultures[5] as well as by mounting evidence for the role of genomic and phenotypic heterogeneity in the evolution and adaptation of tumors.[6–9]

Transcriptional reporters based on the production of chemiluminescence and fluorescence signals have been used successfully in the study of a wide variety of signaling pathways.[10–13] Transcriptional reporters of Wnt/β-catenin signaling have been employed with great success leading to the discovery of several novel regulators of Wnt signaling.[3,1,2,11] Since Wnt/β-catenin signaling culminates in the co-activation of TCF/LEF family members, transcriptional reporters of Wnt/β-catenin signaling typically contain multiple TCF/LEF binding sites upstream of a reporter gene. While transcriptional reporters measure Wnt pathway activation by virtue of the induced activity of downstream transcription factors, direct measurements of signaling activation are also possible by tracking the localization of β-catenin. Immunohistochemical methods permit observation of nuclear accumulation of β-catenin as a readout for Wnt pathway activation[14], however the dynamic range and the strength of the signal can vary widely as Wnt signaling is highly sensitive to changes in nuclear β-catenin levels rather than the absolute amount present.[15] Additionally, staining can only be performed in fixed cells and significant amounts of β-catenin will be present in adherens junctions at the cell membrane making measurement of nuclear concentrations challenging. Fusions of β-catenin and fluorescent proteins enable high-contrast, real-time tracking of signaling in live cells[16]; however, this strategy suffers from many of the same disadvantages of immunohistochemistry with respect to dynamic range and signal strength. In addition, there remains the risk that the fusion protein significantly alters the function and dynamics of protein degradation and translocation due to potential steric hindrance from the addition of the bulky fluorescent protein component. For these reasons, transcriptional reporters of Wnt/β-catenin signaling remains the most widely used method to measure pathway activation in living cells.

Modern techniques for the study of intracellular signaling depend on the availability of robust and rapid measures of intracellular signaling activity. The quantitative biomolecular and biophysical characterization of intracellular signaling is highly dependent on the dynamic range and intensity of the reporter signal. While luminescent reporters (through the use of firefly luciferase as the reporter gene[17]) remain the most sensitive readout for reporter activation, fluorescent protein-based reporters permit measurement of reporter activation in single, live cells.[18] In an attempt to reduce cell-to-cell variability to permit more sensitive

measurements pooled over multiple cells, monoclonal cell lines are often employed for fluorescent reporters.[19–23] Noise from polyclonal variability can also be reduced by averaging measurements over a larger number of cells but this leads to increased reagent consumption, reduced throughput and limited dynamic range. These dynamics and variability of fluorescent transcriptional reporters for β-catenin have not been well characterized in the literature, particularly in the context of the evolution of reporter performance in monoclonal cell lines.

This study presents a detailed characterization of a β-catenin activated reporter driving expression of a nuclear localization signal tagged red fluorescent protein (BAR-mCherry) in A375, a cell line derived from human melanoma[24] that does not exhibit abnormal nuclear accumulation of β-catenin.[25] The dynamics of BAR-mCherry activation and relaxation were measured in 6 monoclonal cell lines expanded from single isolated A375-BAR-mCherry cells. A parallel clonogenic assay was implemented using microfabricated cell arrays to characterize the emergence of heterogeneous reporter activation over time-scales significantly shorter than that required to expand single cells into monoclonal cell lines. A detailed study of the dynamics of transcriptional reporter activation in monoclonal populations would be of significant value in the design and optimization of assays utilizing similar reporter systems. Additionally, parallel clonogenic screening of reporter cell line colonies may shed light on the mechanisms by which reporter cell lines evolve and enable the generation of more stable and uniform reporter libraries.

Materials and Methods

Plasmids, Cell Culture and Transfection

A375 human melanoma cells were sourced from the American Type Culture Collection (ATCC). pSL9-BAR-NLS-mCherry was made by mutating pSL9-BAR-Luciferase using site directed mutagenesis to allow for subcloning of NLS-mCherry. The NLS-mCherry construct was a gift of Jon Lane. A375 cells were infected with pSL9-BAR-NLS-mCherry as described previously and will be referred to as A375-BAR-mCherry for brevity.[13] Cells were cultured in Dulbecco's Modified Eagle Medium (DMEM, Life Technologies, Carlsbad, CA) with 10% fetal bovine serum (FBS, Thermo Scientific, Waltham, MA), 500 ng / mL gentamicin sulfate and 250 ng / mL amphotericin B (Life Technologies, Carlsbad, CA).

Conditioned Media and Reagents

Control and Wnt-3a transfected L-cells were obtained from the ATCC and conditioned media was prepared according to ATCC protocol. Murine recombinant Wnt-3a was purchased from Sigma-Aldrich and reconstituted at 1 mg/mL in deionized (DI) water with 0.1% bovine serum albumin and stored in aliquots at −80 °C. Aliquots were thawed and diluted further with phosphate buffered saline (PBS; 137 mM NaCl, 10 mM Na_2HPO_4, 27 mM KCl, 1.75 mM KH_2PO_4, pH 7.4) and used immediately. The GSK3β inhibitor CT 99021 (CHIR 99021, Axon Medicinal Chemistry, Vienna, VA) was stored as a 10 mM solution in DMSO at −20 °C.

Cell Cloning Using Arrays of Releasable Microstructures

Single A375-NLS-mCherry cells were isolated and expanded using arrays of releasable microstructures as a cloning platform (detailed methods provided in supplement).[26] The arrays were sterilized by rinsing with 70% ethanol and air-drying prior to use. A suspension of 4,000 A375-NLS-mCherry cells was seeded into two arrays and incubated for 16 h to allow the cells to adhere. After 16 h the media was exchanged and replaced with 1:1 Wnt-3a conditioned media and fresh DMEM and incubated for 36 h. After 36 h the arrays were stained with 500 ng/mL Hoechst 33342 in PBS for 15 min which was then replaced with fresh DMEM. The array was moved to an inverted microscope (TE-2000-U, Nikon Instruments Inc. Melville, NY) mounted with a custom fabricated collar to hold a 150 μm diameter needle (Roboz Surgical Instrument Co. Gaithersburg, MD) above the 4× objective. Array elements containing a single cell (as identified by the presence of a single fluorescent nucleus in the Hoechst channel) that exhibited strong reporter activation (nuclear localization of mCherry fluorescence) were dislodged from the array as described previously.[26] The released, magnetic microstructures were collected individually with a permanent magnet and transferred to separate wells in a 96-well plate, each containing 100 μL of expansion media (50% A375 conditioned media, 25% fresh DMEM and 25% FBS). A375 conditioned media was prepared by sterile filtering 20 mL of DMEM which had been overlaid on a T75 flask seeded with A375 cells at 50% confluence and aspirated after incubation for 48 h. Media was exchanged every 72 h until expanding colonies greater than 1 mm in diameter were observed. The colonies were then released with 0.15% trypsin and transferred to a 6-well plate for further expansion in standard DMEM. After 3 weeks of total expansion, cells were present at sufficient density to passage and aliquots were cryopreserved in FBS with 10% DMSO. A total of 6 monoclonal cell lines were generated and maintained for characterization. Fresh aliquots of monoclonal cells were used for at least 1 passage after thawing and within 3 passages after thawing.

Single Cell Tracking and Reporter Dynamics Measurement

All 6 monoclonal A375-BAR-mCherry cell lines were screened on 3 cell culture substrates: tissue culture treated polystyrene (TC), fibronectin (Fbn) and gelatin (Gel). To prepare the fibronectin-coated surface, wells of a tissue culture treated 96-well plate were incubated at 25 °C in 50 μL of 20 μg/mL of human plasma fibronectin (EMD Millipore, Billerica, MA) for 1 h then rinsed 3× with PBS before use. Gelatin coated wells were prepared by incubating at 25 °C in 0.1% gelatin in water (EMD Millipore) for 1 h, then rinsed 3× with PBS before use. 1000 cells from each monoclonal line were seeded into two wells each with identical surface treatments containing 100 μL of DMEM and incubated for 16 h to allow the cells to adhere and stabilize. The media was aspirated and replaced with 50 μL of DMEM with 1 μg/mL of recombinant Wnt-3a and 250 ng/mL of Hoechst 33342 and incubated at 37 °C for 2 h. In control wells, media was replaced with DMEM containing 250 ng/mL of Hoechst 33342 and a volume of 0.1% BSA in water identical to the volume added in media containing Wnt-3a. After 2 h the media was aspirated, the wells rinsed gently 3× with warm PBS (37 °C) and replaced with 100 μL of fresh DMEM and 250 ng/mL of Hoechst 33342. The 96-well array was then transferred to an inverted microscope (IX-81, Olympus America, Center Valley, PA) enclosed in a custom fabricated black Delrin housing with temperature, humidity (AirTherm ATX-H, World Precision Instruments, Sarasota, FL)

and CO_2 ($ProCO_2$, BioSpherix, Lacona, NY) regulation maintained at 37 °C, 60% relative humidity and a 5% CO_2 atmosphere. The inverted microscope was outfitted with a motorized XY stage (MS-2000, Applied Scientific Instrumentation, Eugene, OR), a metal arc lamp excitation source (Lumen 200, Prior Scientific, Rockland, MA), high speed shutter (Lambda 10-2, Sutter Instrument Company, Novato, CA) and cooled interline CCD camera (CoolSnap HQ2, Photometrics, Tucson, AZ). Multiple positions within each well were imaged at 10× magnification in the Hoechst and mCherry channels every 10 min for 62 h using the multidimensional acquisition tool in the open source microscope control software, Micro-Mananger.[27] A reference well was seeded with beads containing a fluorescent standard (MultiSpeck, Life Technologies) and was also imaged every 10 min in both channels.

The Hoechst channel image at each position and time-point was segmented using a custom pipeline implemented in CellProfiler[28]. Briefly, background fluorescence in the image was estimated by grayscale morphological opening and subtracted from the original image. The image was then smoothed with a 6 pixel median filter to reduce over segmentation of nuclei. The smoothed image was then converted to a black and white image with a threshold determined by the two-class implementation of Otsu's method[29] and segmented nuclei were declumped using a watershed method based on the shape of the detected nuclei. The segmented images were then exported with each object labeled by a 16-bit integer number for tracking. A custom tracking script was implemented in MATLAB (The Mathworks Inc. Natick, MA) using the overlap method. Briefly, the intersection of every time-adjacent pair of images was calculated and nuclei in each image were assigned a shared label with the segmented nuclei from the previous time-point with which it shared the largest overlap. A second search was implemented to identify nuclei which shared no overlap with a nucleus in a previous time-point by searching for unmatched nuclei within a 20 μm neighborhood from the detected nucleus' position. In cases where no match was found by overlap or distance (for example when a cell migrated from outside of the field of view), a new label was generated and used to track that object in subsequent frames although measurements were only made for cells that could be tracked uninterrupted over all time-points. The labeled images of cell nuclei were then dilated by 5 pixels and used to integrate fluorescence in the mCherry channel for each corresponding nucleus at each time-point. Images of the reference well containing fluorescence standard beads were segmented in both channels using an empirical threshold and the mean fluorescence density (object intensity / object area in pixels) of the beads in each channel were measured at each time-point to control for variations in arc lamp intensity.

Array Scan Automation

Microfabricated arrays were scanned using an automated software utility that provided a customized interface to the μManager microscope control libraries. Array scanning required four steps: user input of the array geometry (number of rows and columns, array element dimensions), user-assisted localization of 2 opposing or 3 adjacent array corners, user-assisted focus at 4 or more positions in the array to calculate the plane of best fit and the sequential imaging of each field of view within the array. Images from each field of view were segmented based on the position of each microstructure which was calculated by

interpolating from the user-identified corner positions and images of each individual microstructure were saved separately for image analysis.

Clonogenic Screening

Microfabricated cell arrays (110×110 array, rows × columns, 200×200×35 μm elements, length × width × height) were fabricated and prepared as previously described (detailed methods provided in supplement).[30,31] For clonogenic screening, the arrays were mounted in custom cassettes fabricated by 3D printing polylactic acid with a convention fusion deposition modeling printer (BFB-3000, Bits from Bytes Ltd, now 3D Systems Inc. Rock Hill, SC) by gluing with a small amount of PDMS. The mounted arrays were sterilized by rinsing with 75% ethanol in water and air-dried prior to coating with fibronectin. The fibronectin coating was prepared by incubating the arrays in 20 μg/mL fibronectin in PBS for 2 h at 25 °C. The arrays were then rinsed 3× with PBS and immediately seeded with cells.

A total of 3,000 cells from the polyclonal A375-BAR-mCherry line were seeded onto each of 4 arrays and incubated for 16 h. After 16 h, the media was exchanged and the cells were incubated in 500 ng/mL of Hoechst 33342 in DMEM for 15 min at 37 °C and rinsed 3× with PBS. Two arrays were overlaid with DMEM containing 1 μg/mL of recombinant Wnt-3a and 2 arrays were overlaid with DMEM containing 5 μM CT 99021. The arrays were immediately scanned at 4× magnification to measure Hoechst and basal mCherry fluorescence. After scanning, the arrays were incubated for 36 h at 37 °C, rinsed 3× with PBS and incubated in DMEM containing 500 ng/mL of Hoechst 33342 in DMEM for 15 min at 37 °C. The arrays were again rinsed 3× with PBS and immediately scanned. After an additional 36 h, the arrays were re-stained with Hoechst 33342, rinsed and the media was replaced prior to scanning. The media was exchanged 48 h later but the arrays were not scanned. A total of 5 d after the previous scan and after single cells on the array had expanded into colonal colonies, the media was exchanged, the arrays stained with Hoechst 33342, and overlaid with solutions of recombinant Wnt-3a and CT 99021 as described above and the arrays were again scanned. After 36 h, the arrays were rinsed, stained and overlaid with DMEM prior to the final scan. Images from scanned arrays were segmented using the CellProfiler pipeline described above with parameters empirically adjusted to account for the higher background fluorescence from the photoresist substrate and lower magnification of the images. The integrated mCherry fluorescence was processed in terms of fluorescence density (RFU / pixel) using MATLAB since the mean fluorescence density of a colony will not be affected by under or over-segmentation errors caused by densely clustered cell nuclei. The purity of monoclonal colonies was assessed by manually inspecting the images of 25 microstructures on each array which had at least 2 adjacent microstructures with no cells at the first time-point of the experiment.

Results and Discussion

Description of BAR-mCherry Reporter

Monoclonal cell lines are widely utilized in quantitative biomolecular and biophysical assays in an attempt to reduce biological variability as a source of noise.[19–23] The generation

of monoclonal cell lines requires the expansion of single cells over tens of generations to provide a sufficiently large number of cells to process using conventional tissue culture techniques. The evolution of monoclonal cell lines over these timescales has not been well characterized. To characterize a reporter system in monoclonal cell lines, A375 cells were infected with a β-catenin activated reporter (BAR) driving expression of a nuclear localization signal-tagged mCherry red fluorescent protein (NLS-mCherry). The BAR-mCherry reporter utilizes 12× TCF/LEF binding sites upstream of an NLS-tagged mCherry construct to function as a readout for Wnt/β-catenin signaling (Figure 1A). In A375-BAR-mCherry cells, NLS-mCherry is not produced at levels detectable by fluorescence microscopy (Figure 1B) until treatment with Wnt3A ligand (Figure 1C). The nuclear localization signal leads to accumulation of mCherry in the nucleus, simplifying automated image analysis as only segmentation of the nucleus is required to quantify mCherry fluorescence.

Variability in Wnt Signaling Reporter Activity

Six monoclonal cell lines were generated from a polyclonal population of A375 cells transfected with BAR-mCherry for the characterization of reporter dynamics. These clones were expanded over multiple generations (3 weeks, >25 generations) on a conventional polystyrene surface to populations large enough to be passaged and manipulated conventionally and the dynamics of reporter activation were measured at the single cell level within each clone. Cells were tracked for 62 h with or without a brief treatment of recombinant Wnt-3a (1 μg/mL, 2 h). The production of mCherry over time was measured from a total of 1,895 treated cells (Figure S1) and 781 untreated cells (Figure S2) cultured on polystyrene by fluorescence microscopy and single-cell tracking.

Significant variability was observed in both the kinetics (Figure 2A) and magnitude (Figure 2B) of Wnt reporter activation between A375-BAR-mCherry clones, however the magnitude of activation (12 pair-wise differences, $p < 0.01$, p-values listed in Table S1) was seen to vary more between clones than the kinetics of activation (6 pair-wise differences, $p < 0.01$, p-values listed in Table S2). Clone 2 was observed to be the most unique of all 6, showing significant differences in the median magnitude of activation and the time to reach peak activation relative to all other clones tested. Clones 1, 3, 5 and 6 exhibited pairwise differences in their median peak magnitude of activation between all but one other clone with similarities observed between clones 1 and 3 and clones 5 and 6. The kinetics of activation varied minimally in clones 2 through 6, with the only additional pair-wise difference existing between clones 2 and 4. The signal relaxation kinetics of single A375-BAR-mCherry cells, while highly varied ($\mu = 6.5$ h, $\sigma = 5.6$ h), did not exhibit many differences between clones (Figure 2C). Only 2 statistically significant pair-wise differences were observed in the median time for signal to relax to half peak fluorescence ($p < 0.01$, p-values listed in Table S3); between clones 2 and 4 and clones 4 and 6. The activation kinetics, peak activation magnitude and signal relaxation rate of BAR-mCherry are believed to be a function of 3 basic processes: induction of Wnt signaling and activation of the BAR-mCherry reporter, synthesis and nuclear transport of NLS-mCherry and the non-specific proteasomal degradation of NLS-mCherry. In addition to significant intraclonal variability in the magnitude and kinetics of reporter activation and inactivation, the interclonal

variability observed (primarily in peak activation magnitude and to a lesser extent in activation kinetics) is suggestive of the presence of fundamental differences in Wnt signaling, transcriptional, translational and degradation phenotypes between individual monoclonal cell lines.

Variations in Reporter Dynamics Are Regulated by Independent Processes

Hoechst fluorescence, a measure of DNA concentration, and reporter activation kinetics were not correlated with reporter activation magnitude for any individual clone (Table S4) or for the measurements of all clones pooled together (Figure 3A, B). The nuclear size and Hoechst fluorescence intensity of cells was observed to vary significantly even within monoclonal populations, suggestive of aneuploidy. Wnt signaling is modulated during the cell cycle[32,33], however it is not possible to correlate progression through the cell cycle with DNA concentration in an aneuploid population. In comparing the mean intensity of nuclear Hoechst fluorescence over the course of the experiment against the peak activation magnitude (Figure 3A), no correlation between the two measurements was seen for any of the clones ($r^2 = 0.09$). Thus the amount of DNA present in each cell did not appear to influence the magnitude of reporter activation and the magnitude of reporter activation was independent of DNA content or degree of aneuploidy. The kinetics of activation (as measured by the time require to reach peak fluorescence intensity) were also uncorrelated with the magnitude of activation ($r^2 = 0.15$; Figure 3B). While the rate of signal accumulation varied significantly from cell-to-cell, it was not dependent on or influenced by the activation magnitude of the reporter. This suggests that the rate and magnitude of reporter activation were regulated by distinct processes. It is likely that the rate of signal accumulation was a function of the kinetics of NLS-mCherry translation and degradation while the magnitude of reporter activation was a function of the fold-change in the nuclear concentration of β-catenin.[15] The signal relaxation kinetics of all 6 clones varied widely from cell to cell, but was observed to be uncorrelated with either peak activation magnitude (Figure 3C, $r^2 = 0.01$) or the time required to reach peak activation (Figure 3D, $r^2 = 0.006$). In tumor cells, non-specific proteasomal degradation likely dictates the reporter signal decay rate due to the critical role protein degradation plays in survival.[34–36] In totality, these observations strongly support the interpretation that the kinetics of reporter activation, the magnitude of reporter activation and the kinetics of signal relaxation were independently regulated and highly variable processes in A375-BAR-mCherry. While we could not test for correlations between cell cycle and reporter activation magnitude, Hoechst fluorescence, a measure of DNA concentration was not correlated with reporter activation magnitude.

Matrix-dependence of Wnt/β-catenin Reporter Activation

The influence of extracellular matrix (ECM) mediated signaling on the reporter phenotype was also characterized for each clone as a potential indicator of inter-clonal phenotypic variability as integrin signaling is known to promote Wnt activity.[37–40] Differential integrin binding to polystyrene, gelatin and fibronectin surfaces was expected to produce different degrees of reporter modulation in cells treated with Wnt. Three culture substrates were evaluated: tissue-culture polystyrene, human-plasma fibronectin, and gelatin. Cells cultured on each substrate were tracked for 62 h with or without a brief treatment of recombinant Wnt-3a (1 μg/mL, 2 h). The production of mCherry over time was measured from a total of

5,598 treated cells (Figure S1) and 2,647 untreated cells (Figure S2) by fluorescence microscopy and single-cell tracking. Reporter activation kinetics, peak activation magnitude and signal relaxation kinetics for cells cultured on fibronectin and gelatin were observed to be similarly uncorrelated as compared to cells cultured on polystyrene (Figure S3A-C). Reporter activation magnitude was also similarly uncorrelated with mean Hoechst fluorescence (Figure S3D). This further reinforces our conclusion that these components of overall reporter dynamics are independent of each other as well as of ECM-mediated effects on Wnt signaling in A375-BAR-mCherry.

While significant intraclonal heterogeneity was present in all clones on all cell culture substrates in terms of reporter activation kinetics (Figure 4A) and relaxation kinetics (Figure 4C), the ECM did not possess a strong impact on these attributes in most clones. In terms of reporter kinetics, activation rates (Figure 4A) exhibited a dependence on cell culture substrate in only two clones ($p < 0.01$, p-values listed in Table S5), while signal relaxation rates (Figure 4C) exhibited no dependence on ECM interactions ($p < 0.01$, p-values listed in Table S6). Within clones 3 and 4, a statistically significant difference was observed in the time required to reach peak mCherry fluorescence between cells cultured on fibronectin and cells cultured on gelatin. Within clone 4, a difference was also observed in the time required to reach peak fluorescence between cells cultured on polystyrene and cells cultured on gelatin. The presence of only 3 statistically significant pair-wise differences out of 12 comparisons in the dependence of reporter activation kinetics on ECM interactions demonstrated that that intraclonal variability in reporter activation and signal relaxation kinetics was generally much greater than the variability caused by ECM-dependent interactions.

In contrast to activation and relaxation kinetics, reporter activation magnitude was observed to depend on cell culture substrate (Figure 4A) with significant variations in magnitude both within and between clones (12 pair-wise differences out of 18 comparisons, $p < 0.01$, p-values listed in Table S7). For clones 1–3, cells cultured on fibronectin reached a significantly higher peak fluorescence intensity ($p < 0.01$, p-values listed in Table S8) than on polystyrene or gelatin. Clones 4–6 departed from this trend, again suggesting the presence of distinct signaling phenotypes within the A375-BAR-mCherry population from which the clones were selected.

Characterization of Reporter Cell Lines by Clonogenic Screening

The dangers of phenotypic and genetic drift of in-vitro cultured cell lines over time have been widely discussed.[41,42] In light of the time required to expand monoclonal cell lines to sufficient size for manipulation with conventional cell culture techniques, there is some question as to whether the heterogeneity observed in reporter systems for Wnt/β-catenin signaling are inherent to the pathway, artifacts of the reporter, a product of long-term drift or a combination of all three. Regardless of the origins of this diversity, there are significant practical implications for the use of monoclonal cell lines and transcriptional reporters. Studying monoclonal colonies a smaller number of generations removed from the originating mother cell could reduce the impact of long-term phenotypic drift and provide evidence as to the origins of inter- and intra-clonal heterogeneity, but would also reduce the

statistical power of measurements made on the smaller number of cells available. Analyzing a large number of monoclonal colonies in parallel would enable statistical comparisons to be made while also increasing the likelihood of capturing a representative sample of the diverse signaling phenotypes which may be present. To characterize the diversity of monoclonal colonies early in their evolution, we screened a large number of A375-BAR-mCherry clones in a massively parallel fashion using microfabcricated cell arrays.[43–45] With these arrays, cells are prevented from migrating between adjacent microstructures by a long-lived intervening air bubble.[31] The maintenance of clonal isolation was assessed by manually examining 25 microstructures and their neighboring unoccupied microstructures on each of 4 arrays (100 microstructures in total) over 8 days. Across all 100 positions examined and over the 8 days, no cells ever appeared on microstructures that were unoccupied on day 1.

The clonogenic screen consisted of 3 steps: an initial activation assay on single A375-BAR-mCherry cells after 16 h of culture on cell arrays, a 5 day expansion period in which the single cells grew into monoclonal colonies and a final activation assay performed on the monoclonal colonies at day 8 of culture (Figure 5). The activation assays were performed by addition of Wnt-3a or CT99021 (an inhibitor of GSK3β) to the arrayed cells followed imaging of Hoechst and mCherry fluorescence 36 h later. The 5-day expansion period was selected so that colonies could undergo up to 6 rounds of cell division (A375 doubling time is <20 h[46]). By assaying both single A375-BAR-mCherry cells and their clonal progeny, reporter activation of the clones could be correlated to the activity of the mother cell to track divergence. In addition to imaging the arrays for mCherry expression before and after the initial and final activation assays, a scan was performed 36 h after completion of the first activation assay to track signal relaxation; however, no cells were observed to be detectably more fluorescent than basal levels at this time-point. A total of 1,119 clones were assayed over four arrays. Of these, 684 clones were tracked on two arrays treated with Wnt-3a and 435 clones were tracked on two arrays treated with CT 99021.

Evidence of Cell Division-Dependent Wnt Signaling Feedback

On average, daughter cells treated with Wnt-3a (Figure 6A) showed 13.9% lower peak fluorescence relative to their corresponding mother cells. Reporter activation magnitude was observed to vary with the number of cell divisions a colony underwent in A375-BAR-mCherry clones treated with Wnt-3a (Figure 6A, C). Cells which were viable but remained non-proliferative (corresponding to 0 divisions) exhibited significantly ($p < 0.01$) weaker mCherry fluorescence during the second treatment step relative to the first treatment. Cells that did not divide did not exhibit detectably greater basal levels of activation prior to the second treatment. This observation directly supports previous evidence of the self-inhibition by Wnt/β-catenin pathway activation[47] (Figure 1A). Multiple downstream gene targets of β-catenin include Wnt signaling inhibitors such as DKK[48], which causes Frizzled receptor internalization, β-transducin repeat containing protein[49] (β-TrCP), which mediates ubiquitination of phosphorylated β-catenin, and Axin2[50], a key scaffold for the destruction complex.

Cell division or associated signaling processes regulate Wnt self-inhibition. Colonies treated with Wnt-3a that underwent multiple cell divisions (>2) exhibited significantly increased

reporter activation levels relative to the overall population (Figure 6C; $p < 0.01$). Cell density has been observed to play a role in the modulation of Wnt signaling, potentially due to cross-talk between the cytosolic and adherens-associated pools of β-catenin.[16] This relationship has been observed to be inhibitory in nature as up-regulation of the formation of adherens-junctions may reduce the cytosolic pool of β-catenin available for Wnt-induced signaling.[51] In contrast, we observed that smaller colonies exhibited a lower level of signaling activation relative to their mother cell while larger colonies exhibited an increase in signaling activation. This sensitization of dense clonal colonies to Wnt-induced signaling is likely a consequence of signaling distinct from the adherens-associated β-catenin pool, of which there are several potential candidates.

A number of positive feedback loops for Wnt pathway activation have been identified with oncogenic implications.[52–55] These feedback loops regulate Wnt signal transduction at both the receptor and destruction complex level and can lead to increased β-catenin expression levels. Additional investigations will be necessary in order to identify the mechanisms underlying the change in colony signaling we observed. Any potential link between positive feedback and cell division remains even less clear, although several of the signaling pathways identified in the literature which feed into Wnt signaling are also tied to proliferative phenotypes including hepatocyte growth factor receptor[56,52] (HGFR), extracellular signal-regulated kinases[53] (ERK), c-Myk[57] and phospholipase D1[55] (PLD1). We speculate that our observed correlation of increased Wnt sensntivity with clonal colonies undergoing multiple divisions (Figure 6C) could represent an effect of increased feedback activity from Wnt signaling partners rather than the cause of sensitization. At least some of the heterogeneity we observed can likely be attributed to epigenetic silencing or activation of reporter integration sites[58], however epigenetic silencing of the reporter should be randomly distributed over a sufficiently large number of sub-clones and should not exhibit a bias that is dependent on the point of pathway activation or cell division.

Inhibition of GSK3β Removes Cell Division-Dependence of Reporter Activation

In A375-BAR-mCherry clones treated with CT99021, reporter activation magnitude was seen to decrease by an average of 8.34% relative to the activation magnitude of the mother cells. Reporter activation magnitude did not vary with the number of divisions a colony underwent (Figure 6B, D). The lack of a trend in clones treated with CT99021 ($p > 0.01$, Figure 6D) agrees with proposed mechanisms of Wnt self-inhibition as this feedback is integrated at or before the level of the destruction complex. Since GSK3β inhibition directly inhibits the function of the destruction complex, desensitization to Wnt by increased expression of DKK, β-TrCP or Axin2 in cells would have no effect on the induction of signaling in cells treated with CT 99021. Positive feedback was also not evident in colonies treated with CT99021 as the distribution of the fold-change in reporter activation magnitude was homogenous with respect to the number of cell divisions each colony underwent (Figure 6D). Since the known mechanisms of Wnt sensitization and positive feedback also function at or upstream of the destruction complex, their effects on reporter activation by treatment with CT 99021 would be expected to have been significantly reduced. While increased β-catenin expression levels might still result in positive feedback, recent evidence suggests that Wnt signaling is defined by a fold-change in nuclear β-catenin concentration, not the

absolute concentration and the magnitude of reporter activation we observed was likely dominated by the activity of CT 99021.[15]

Conclusions

Our observations present a cautionary tale regarding the reliance on monoclonal cell lines as reporter systems for the study of intracellular signaling. Conventional in-vitro reporter-based assays probe simplified systems in which the dynamics of cellular signaling and interactions are suppressed or reduced through strategies such as the generation of monoclonal cell lines, however this is fraught with risk. We observed the selection of distinct signaling phenotypes in the generation of monoclonal cell lines which may represent (or miss) rare subpopulations in the polyclonal population or which may not exist in-vivo. In the characterization of ECM-dependent modulation of reporter activation, we observed significant differences in the pattern of signal enhancement and inhibition between clones. As extracellular signaling is integrated into Wnt signaling through multiple intermediates[37–40], it is possible that these distinct phenotypes may be defined by differences in expression levels or mutations in intermediate signaling cascades or receptor signaling complexes. This is an alarming observation for signaling investigations which rely on monoclonal cell lines as characterization of individual clones with different signaling phenotypes could lead to seemingly contradictory observations. For example, selection of a single clone could provide evidence that fibronectin-mediated integrin signaling enhances Wnt-induced reporter activation (*eg.* clone 1) or, if a different clone had been selected, the same experiments could suggest the opposite relationship (*eg.* clone 5). The use of single monoclonal cell lines should thus be avoided in the study of signaling pathways as phenotypes and interactions identified may vary significantly between different clones, even those prepared from the same cell line, reducing the generalizability of findings and making their replication challenging. We observed reporter activation levels diverge within 5 generations of the isolation of clonal populations over a 2-log range (0.1–10× the relative signal response of the mother cells). This range matches closely with observations in a different biological and reporter system for β-catenin[5], suggesting that our observations are not unique to A375-BAR-mCherry. Single-cell resolution measurements of polyclonal populations are likely a more robust platform for screening and discovery. Combining single-cell measurements with a platform for performing cell isolations, such as arrays of releasable microstructures, would allow sub-populations exhibiting distinct phenotypes to be separated and further studied. This would enable a more robust and complete characterization of heterogeneous samples without bias towards specific phenotypes which may be present.

Our observations strongly support the existence of both positive and negative feedback in Wnt/β-catenin signal activation, at least in the A375 cell line. While further study will be necessary to identify the mechanisms underlying the changing signaling phenotypes that we observed, the correlation of Wnt sensitivity with different colony sizes suggests that cell division or a combination of associated molecular signaling events may play a role in modulating both the negative and positive self-regulation of Wnt signaling. To perform a clonogenic screen on the scale that was presented here by limiting dilution would require an average of 3,042 wells to be seeded, consuming eight 384-well plates, 245.8 mL of media per exchange and 245.8 μg of Wnt-3a. Cell array technology enables the rapid performance

of a massively parallel clonogenic screen with comparatively little reagent consumption; in ideal cases up to a 99.5% reduction in reagent consumption on a per-clone basis relative to well-plate screening (Table S9). Additionally, the ability to sort individual selected clones can be utilized in future studies to trace the mechanisms of emergent heterogeneity as well as in the identification of novel regulators of Wnt signaling.

Our observation of multiple clones with diverse signaling phenotypes within a single cell line (Figure 2A & B) highlights the risks of artificially reducing diversity within a reference population, particularly for tumor cells which are known to host diverse subpopulations.[6,7] High throughput screens[20,21,59], fundamental investigations of intracellular signaling[60,61] and single-cell measurements[8,19] performed using a small number of clones could be dramatically affected by the unintentional selection of distinct phenotypes and their results may prove difficult to reproduce or contradictory to the investigations of other groups as a consequence, despite their accuracy within their respective reference systems.

Supplementary Material

Refer to Web version on PubMed Central for supplementary material.

Acknowledgments

This work was supported by a grant EB012549 (NLA) and a New Innovator Award 1-DP2-OD007149-01 (MBM) from the National Institutes of Health and grants from the state of North Carolina's University Cancer Research Fund (MBM). MPW received support from the National Institutes of Health (T32-CA009156-35).

References

1. Berndt JD, Biechele TL, Moon RT, Major MB. Sci. Signal. 2009; 2(pt4)
2. James RG, Biechele TL, Conrad WH, Camp ND, Fass DM, Major MB, Sommer K, Yi X, Roberts BS, Cleary MA, Arthur WT, MacCoss M, Rawlings DJ, Haggarty SJ, Moon RT. Sci. Signal. 2009; 2:ra25. [PubMed: 19471023]
3. Chung N, Marine S, Smith EA, Liehr R, Smith ST, Locco L, Hudak E, Kreamer A, Rush A, Roberts B, Major MB, Moon RT, Arthur W, Cleary M, Strulovici B, Ferrer M. Assay Drug Dev. Technol. 2010; 8:286–294. [PubMed: 20578927]
4. Major MB, Roberts BS, Berndt JD, Marine S, Anastas J, Chung N, Ferrer M, Yi X, Stoick-Cooper CL, von Haller PD, Kategaya L, Chien A, Angers S, MacCoss M, Cleary Ma, Arthur WT, Moon RT. Sci. Signal. 2008; 1:ra12. [PubMed: 19001663]
5. Vermeulen L, De Sousa E Melo F, van der Heijden M, Cameron K, de Jong JH, Borovski T, Tuynman JB, Todaro M, Merz C, Rodermond H, Sprick MR, Kemper K, Richel DJ, Stassi G, Medema JP. Nat. Cell Biol. 2010; 12:468–476. [PubMed: 20418870]
6. Navin N, Kendall J, Troge J, Andrews P, Rodgers L, McIndoo J, Cook K, Stepansky A, Levy D, Esposito D, Muthuswamy L, Krasnitz A, McCombie WR, Hicks J, Wigler M. Nature. 2011; 472:90–94. [PubMed: 21399628]
7. Almendro V, Marusyk A, Polyak K. Annu. Rev. Pathol. 2013; 8:277–302. [PubMed: 23092187]
8. Hou Y, Song L, Zhu P, Zhang B, Tao Y, Xu X, Li F, Wu K, Liang J, Shao D, Wu H, Ye X, Ye C, Wu R, Jian M, Chen Y, Xie W, Zhang R, Chen L, Liu X, Yao X, Zheng H, Yu C, Li Q, Gong Z, Mao M, Yang X, Yang L, Li J, Wang W, Lu Z, Gu N, Laurie G, Bolund L, Kristiansen K, Wang J, Yang H, Li Y, Zhang X, Wang J. Cell. 2012; 148:873–885. [PubMed: 22385957]
9. Anderson ARA, Weaver AM, Cummings PT, Quaranta V. Cell. 2006; 127:905–915. [PubMed: 17129778]

10. Zaslaver A, Bren A, Ronen M, Itzkovitz S, Kikoin I, Shavit S, Liebermeister W, Surette MG, Alon U. Nat. Methods. 2006; 3:623–628. [PubMed: 16862137]
11. Major MB, Roberts BS, Berndt JD, Marine S, Anastas J, Chung N, Ferrer M, Yi X, Stoick-Cooper CL, von Haller PD, Kategaya L, Chien A, Angers S, MacCoss M, Cleary MA, Arthur WT, Moon RT. Sci. Signal. 2008; 1:ra12. [PubMed: 19001663]
12. Su GH, Sohn TA, Ryu B, Kern SE. Cancer Res. 2000; 60:3137–3142. [PubMed: 10866300]
13. Biechele TL, Adams AM, Moon RT. Cold Spring Harb. Protoc. 2009; 2009 pdb.prot5223.
14. Kobayashi M, Honma T, Matsuda Y, Suzuki Y, Narisawa R, Ajioka Y, Asakura H. Br. J. Cancer. 2000; 82:1689–1693. [PubMed: 10817505]
15. Goentoro L, Kirschner MW. Mol. Cell. 2009; 36:872–884. [PubMed: 20005849]
16. Kam Y, Quaranta V. PLoS One. 2009; 4:e4580. [PubMed: 19238201]
17. Biechele TL, Moon RT. Methods Mol. Biol. 2008; 468:99–110. [PubMed: 19099249]
18. Biechele TL, Camp ND, Fass DM, Kulikauskas RM, Robin NC, White BD, Taraska CM, Moore EC, Muster J, Karmacharya R, Haggarty SJ, Chien AJ, Moon RT. Chem. Biol. 2010; 17:1177–1182. [PubMed: 21095567]
19. Bartfeld S, Hess S, Bauer B, Machuy N, Ogilvie LA, Schuchhardt J, Meyer TF. BMC Cell Biol. 2010; 11:21. [PubMed: 20233427]
20. King KR, Wang S, Irimia D, Jayaraman A, Toner M, Yarmush ML. Lab Chip. 2007; 7:77–85. [PubMed: 17180208]
21. Ji LL, Sheng YC, Chen L, Wang ZT. Drug Discov. Ther. 2009; 3:2–5. [PubMed: 22495460]
22. Durocher Y, Perret S, Thibaudeau E, Gaumond MH, Kamen A, Stocco R, Abramovitz M. Anal. Biochem. 2000; 284:316–326. [PubMed: 10964415]
23. Li X, Shen F, Zhang Y, Zhu J, Huang L, Shi Q. Eur. J. Pharm. Biopharm. 2007; 67:284–292. [PubMed: 17337170]
24. Giard DJ, Aaronson SA, Todaro GJ, Arnstein P, Kersey JH, Dosik H, Parks WP. J. Natl. Cancer Inst. 1973; 51:1417–1423. [PubMed: 4357758]
25. Widlund HR, Horstmann MA, Price ER, Cui J, Lessnick SL, Wu M, He X, Fisher DE. J. Cell Biol. 2002; 158:1079–1087. [PubMed: 12235125]
26. Wang Y, Phillips C, Xu W, Pai J-H, Dhopeshwarkar R, Sims CE, Allbritton N. Lab Chip. 2010; 10:2917–2924. [PubMed: 20838672]
27. Edelstein A, Amodaj N, Hoover K, Vale R, Stuurman N. Chapter 14. Curr. Protoc. Mol. Biol. 2010 Unit14.20.
28. Carpenter AE, Jones TR, Lamprecht MR, Clarke C, Kang IH, Friman O, Guertin DA, Chang JH, Lindquist RA, Moffat J, Golland P, Sabatini DM. Genome Biol. 2006; 7:R100. [PubMed: 17076895]
29. Otsu N. IEEE Trans. Syst. Man. Cybern. 1979; 9:62–66.
30. Shah PK, Hughes MR, Wang Y, Sims CE, Allbritton NL. J. Micromechanics Microengineering. 2013; 23:107002.
31. Wang Y, Bachman M, Sims CE, Li GP, Allbritton NL. Anal. Chem. 2007; 79:7104–7109. [PubMed: 17705452]
32. Hadjihannas MV, Bernkopf DB, Brückner M, Behrens J. EMBO Rep. 2012; 13:347–354. [PubMed: 22322943]
33. Davidson G, Shen J, Huang Y-L, Su Y, Karaulanov E, Bartscherer K, Hassler C, Stannek P, Boutros M, Niehrs C. Dev. Cell. 2009; 17:788–799. [PubMed: 20059949]
34. Adams J. Drug Discov. Today. 2003; 8:307–315. [PubMed: 12654543]
35. Almond JB, Cohen GM. Leukemia. 2002; 16:433–443. [PubMed: 11960320]
36. Adams J, Palombella VJ, Elliott PJ. Invest. New Drugs. 2000; 18:109–121. [PubMed: 10857991]
37. Liu Y, Chattopadhyay N, Qin S, Szekeres C, Vasylyeva T, Mahoney ZX, Taglienti M, Bates CM, Chapman HA, Miner JH, Kreidberg JA. Development. 2009; 136:843–853. [PubMed: 19176588]
38. Crampton SP, Wu B, Park EJ, Kim J-H, Solomon C, Waterman ML, Hughes CCW. PLoS One. 2009; 4:e7841. [PubMed: 19924227]

39. Olivares-Navarrete R, Hyzy SL, Park JH, Dunn GR, Haithcock DA, Wasilewski CE, Boyan BD, Schwartz Z. Biomaterials. 2011; 32:6399–6411. [PubMed: 21636130]
40. De Toni F, Racaud-Sultan C, Chicanne G, Mas VM-D, Cariven C, Mesange F, Salles J-P, Demur C, Allouche M, Payrastre B, Manenti S, Ysebaert L. Oncogene. 2006; 25:3113–3122. [PubMed: 16407823]
41. Hughes P, Marshall D, Reid Y, Parkes H, Gelber C. Biotechniques. 2007; 43:575–586. [PubMed: 18072586]
42. Masters JR. Nat. Rev. Mol. Cell Biol. 2000; 1:233–236. [PubMed: 11252900]
43. Wang Y, Young G, Aoto PC, Pai J-H, Bachman M, Li GP, Sims CE, Allbritton NL. Cytometry. A. 2007; 71:866–874. [PubMed: 17559133]
44. Quinto-Su, Pa; To'a Salazar, G.; Sims, CE.; Allbritton, NL.; Venugopalan, V. Anal. Chem. 2008; 80:4675–4679. [PubMed: 18489124]
45. Salazar GT, Wang Y, Young G, Bachman M, Sims CE, Li GP, Allbritton NL. Anal. Chem. 2007; 79:682–687. [PubMed: 17222037]
46. Martinez EJ, Owa T, Schreiber SL, Corey EJ. Proc. Natl. Acad. Sci. 1999; 96:3496–3501. [PubMed: 10097064]
47. Piddini E, Vincent J-P. Cell. 2009; 136:296–307. [PubMed: 19167331]
48. Hoang BH. Cancer Res. 2004; 64:2734–2739. [PubMed: 15087387]
49. Latres E, Chiaur DS, Pagano M. Oncogene. 1999; 18:849–854. [PubMed: 10023660]
50. Jho, E-h; Zhang, T.; Domon, C.; Joo, C-K.; Freund, J-N.; Costantini, F. Mol. Cell. Biol. 2002; 22:1172–1183. [PubMed: 11809808]
51. Nelson WJ, Nusse R. Science. 2004; 303:1483–1487. [PubMed: 15001769]
52. Rasola A, Fassetta M, De Bacco F, D'Alessandro L, Gramaglia D, Di Renzo MF, Comoglio PM. Oncogene. 2007; 26:1078–1087. [PubMed: 16953230]
53. Kim D, Rath O, Kolch W, Cho K-H. Oncogene. 2007; 26:4571–4579. [PubMed: 17237813]
54. Kapinas K, Kessler C, Ricks T, Gronowicz G, Delany AM. J. Biol. Chem. 2010; 285:25221–25231. [PubMed: 20551325]
55. Kang DW, Lee S-H, Yoon JW, Park W-S, Choi K-Y, Min DS. Cancer Res. 2010; 70:4233–4242. [PubMed: 20442281]
56. Monga SPS, Mars WM, Pediaditakis P, Bell A, Mule K, Bowen WC, Wang X, Zarnegar R, Michalopoulos GK. Cancer Res. 2002; 62:2064–2071. [PubMed: 11929826]
57. Cho J-H, Dimri M, Dimri GP. J. Biol. Chem. 2013; 288:3406–3418. [PubMed: 23239878]
58. Hoeben RC, Migchielsen AA, van der Jagt RC, van Ormondt H, van der Eb AJ. J. Virol. 1991; 65:904–912. [PubMed: 1702844]
59. Lecault V, Vaninsberghe M, Sekulovic S, Knapp DJHF, Wohrer S, Bowden W, Viel F, McLaughlin T, Jarandehei A, Miller M, Falconnet D, White AK, Kent DG, Copley MR, Taghipour F, Eaves CJ, Humphries RK, Piret JM, Hansen CL. Nat. Methods. 2011; 8:581–586. [PubMed: 21602799]
60. Mueller DL, Jenkins MK, Schwartz RH. J. Immunol. 1989; 142:2617–2628. [PubMed: 2522963]
61. Cloutier J-F, Veillette A. J. Exp. Med. 1999; 189:111–121. [PubMed: 9874568]

Insight, innovation, integration

This work integrates microfabricated cell arrays with automated imaging cytometry and image analysis to generate insight into the evolution of transcriptional reporters. Automated imaging of microfabricated cell arrays enabled massively parallel screening and robust tracking of >1,000 clonal cell colonies to observe emergent signaling phenotypes and heterogeneity. These observations provide insight into Wnt-3a signaling dynamics and highlight challenges facing the use of monoclonal cell lines as reporter systems in cell signaling assays and high throughput screening.

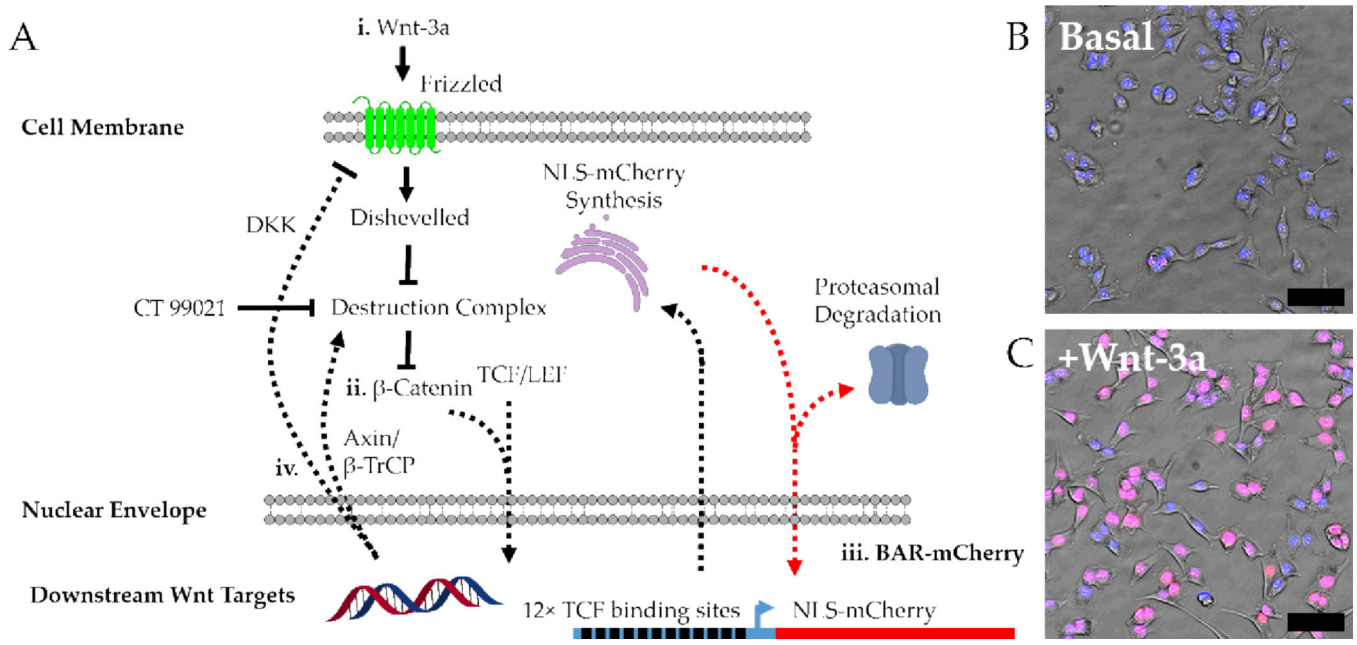

Figure 1.

(A) Simplified schematic of BAR-mCherry integration into the canonical Wnt/β-catenin signaling cascade. (i) Wnt-3a binding to Frizzled results in inhibition of the destruction complex. (ii) β-catenin translocated to the nucleus drives gene expression in concert with TCF/LEF transcription factors. (iii) BAR-mCherry is produced from active β-catenin signaling and builds up as long as production exceeds degradation. (iv) Downstream targets of Wnt include several of its own regulators including Axin and β-TrCP which mediate β-catenin degradation and DKK which causes Frizzled receptor internalization. Example images showing A375-BAR-mCherry cells treated with L-cell conditioned media (no Wnt-3a) (B) and Wnt-3a conditioned media (C) for 24 h. Nuclei are counterstained with Hoechst 33342 (blue) to show nuclear localization of NLS-mCherry (red, merge = pink). Scale bar is 100 μm.

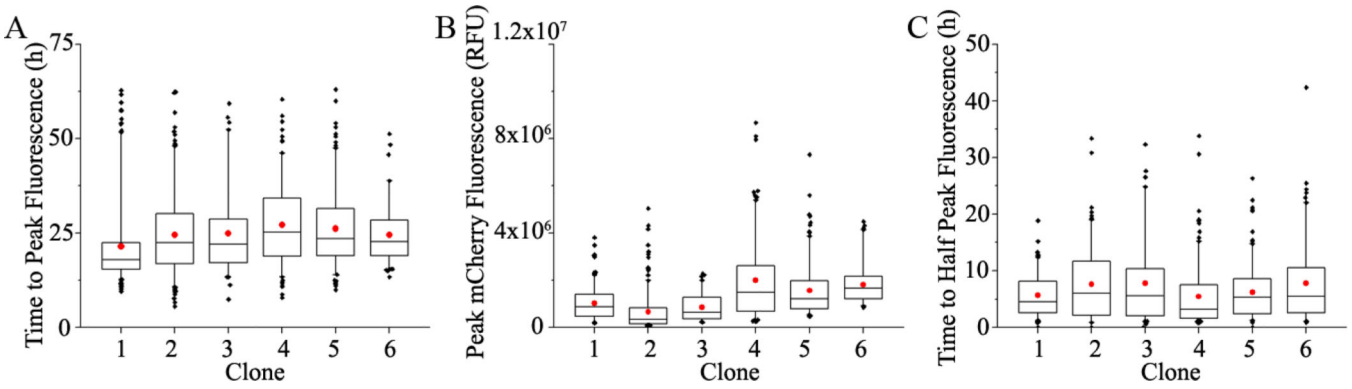

Figure 2.

Box and whisker plots showing the distribution of (A) times required to reach peak fluorescence, (B) the peak mCherry fluorescence achieved and (C) the time required for signal to decay to half peak fluorescence for single A375-BAR-mCherry cells cultured on polystyrene. Red circles mark the population mean for each distribution. Outliers shown are observations above the 5th and below the 95th percentile. The boxes mark the 25th, 50th (median) and 75th percentiles within the distribution while the whiskers mark the 5th and 95th percentiles.

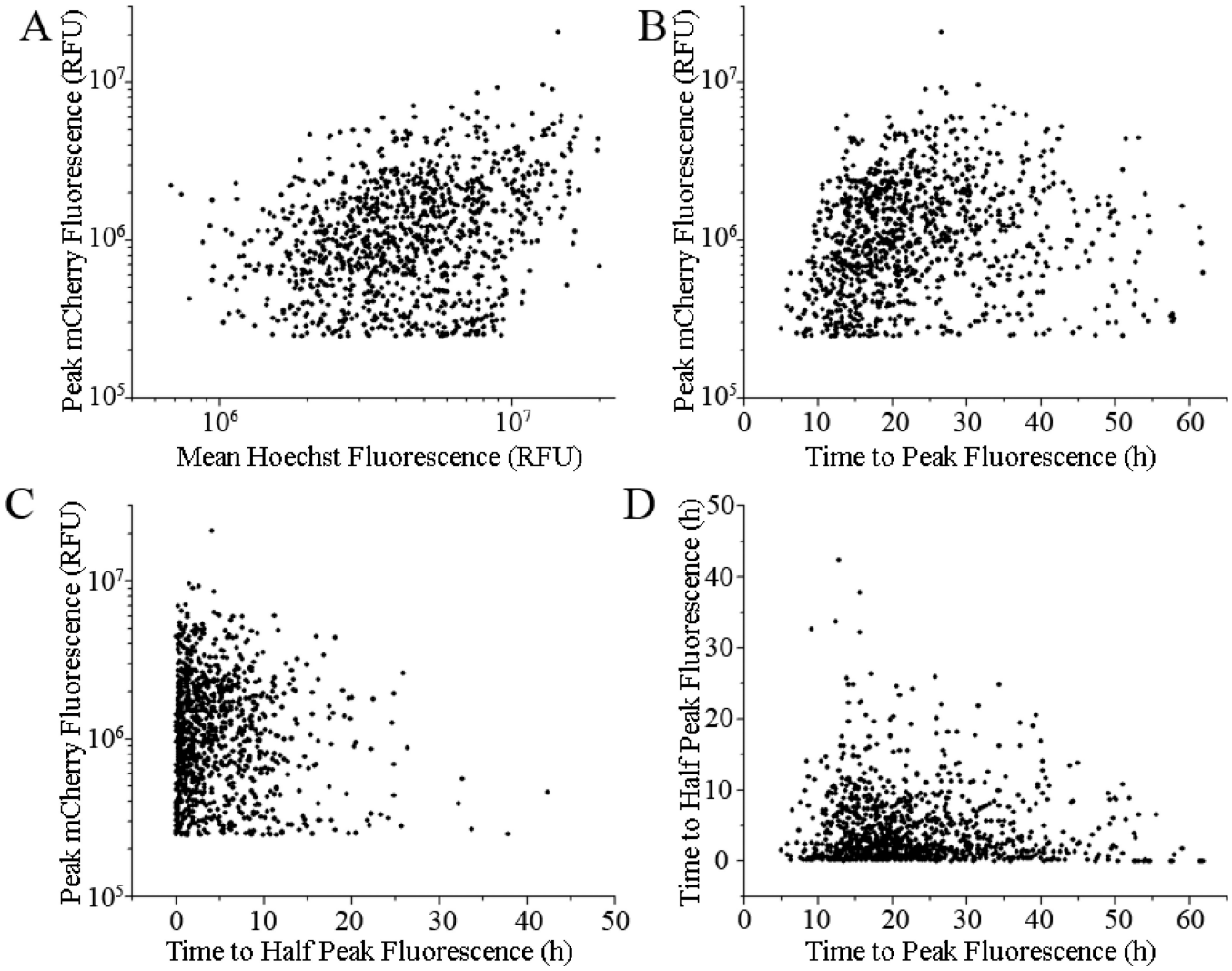

Figure 3.

Comparisons between measured parameters from single-cell tracking of A375-BAR-mCherry cells (all 6 clones are shown pooled together) cultured on polystyrene after treatment with Wnt3a. (A) Peak mCherry fluorescence achieved versus the mean Hoechst fluorescence over the 62 h time-course ($r^2 = 0.09$) (B) Peak mCherry fluorescence versus the time required to reach peak fluorescence ($r^2 = 0.15$) (C) Peak mCherry fluorescence achieved versus the time required for signal to decay to half peak fluorescence ($r^2 = 0.01$) (D) The time required for signal to decay to half peak fluorescence versus the time required for cells to reach peak fluorescence ($r^2 = 0.006$).

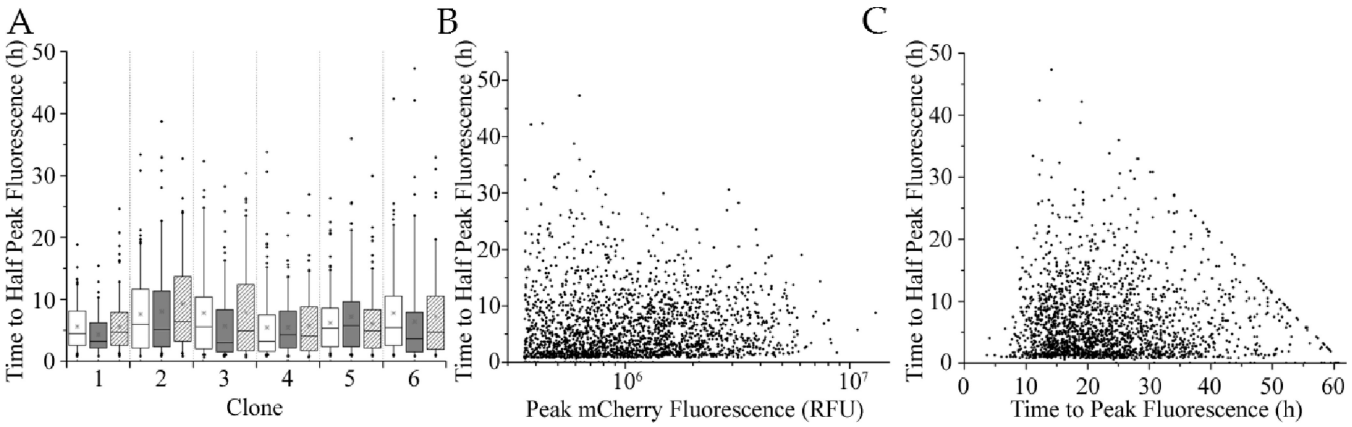

Figure 4.

Box and whisker plots showing the distributions of (A) the times to reach peak mCherry fluorescence, (B) the peak mCherry fluorescence intensity achieved and (C) the time required for signal to decay to half peak mCherry fluorescence for single A375-BAR-mCherry cells cultured on polystyrene (clear boxes), fibronectin (dark gray boxes) and gelatin (diagonal striped boxes). Red circles mark the population mean for each distribution. Outliers shown are observations above the 5th and below the 95th percentile. The boxes mark the 25th, 50th (median) and 75th percentiles within the distribution while the whiskers mark the 5th and 95th percentiles.

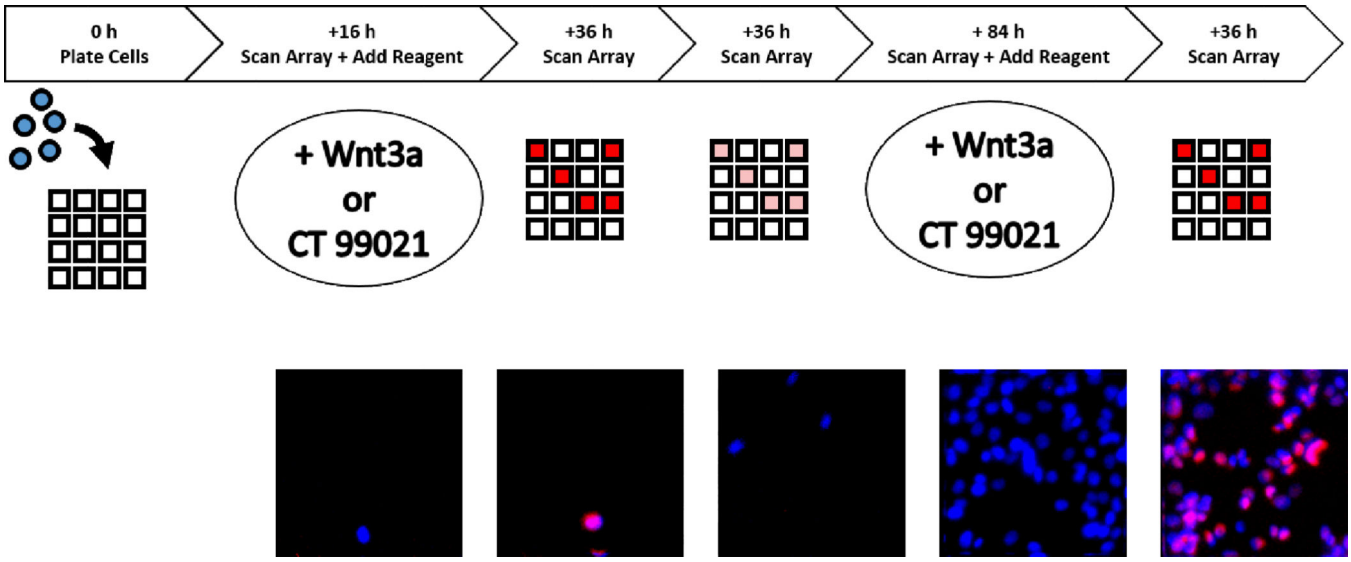

Figure 5.

Process flow for the parallel clonogenic screen on the arrays. The experiment begins by seeding a single cell suspension of A375-BAR-mCherry cells onto the arrays. After 16 h the arrays are scanned to measure basal mCherry expression and then treated with either Wnt-3a or CT 99021. 36 h after treatment, the array is washed and scanned again to measure peak mCherry fluorescence activation. After an additional 36 h, the array is again scanned to track the relaxation of the mCherry signal. 84 h following the relaxation scan, the array is again scanned to confirm that the cells have reached basal activation levels and treated again with Wnt-3a or CT 99021. 36 h post-treatment, the arrays are washed and scanned again to measure peak mCherry fluorescence. Shown below the process flow is a series of images taken of a single clone over the course of the experiment. Hoechst 33342 and mCherry fluorescence is shown in blue and red, respectively.

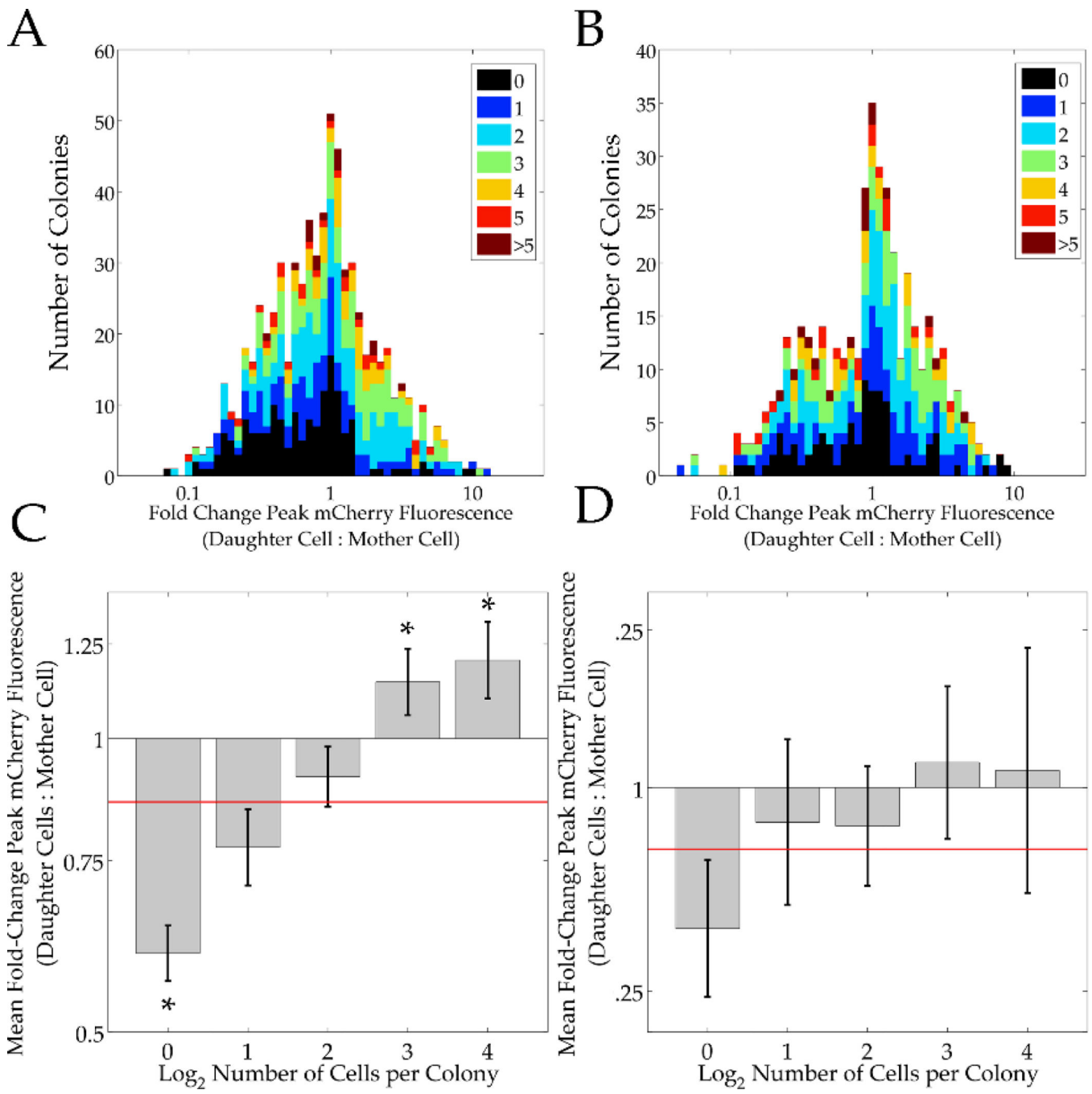

Figure 6.

Distribution of the mean fold change in fluorescence density (RFU / pixel) between each clonal colony in the final time point and its corresponding mother cell for arrays treated with (A) Wnt-3a and (B) CT 99021. The bar color marks the nearest whole number of divisions each clonal colony underwent. Bar charts showing the mean fold-change for cells in each corresponding number of divisions for cells treated with (C) Wnt-3a and (D) CT 99021. Error bars show the standard error of the mean. Red line marks the total population mean. Asterisks mark populations found to be significantly different from the population mean ($p <$

0.01). Bars are not shown for colonies with >4 divisions due to an insufficient number of colonies greater than that size.